Oncolytic Semliki Forest Virus Vector as a Novel Candidate against Unresectable Osteosarcoma

Anna Ketola,[1] Ari Hinkkanen,[5] Felicitas Yongabi,[1] Petra Furu,[5] Ann-Marie Määttä,[1] Timo Liimatainen,[1] Risto Pirinen,[3] Marko Björn,[1] Tanja Hakkarainen,[1] Kimmo Mäkinen,[2,4] Jarmo Wahlfors,[1,4,6] and Riikka Pellinen[1]

[1]A. I. Virtanen Institute for Molecular Sciences, Department of Biotechnology and Molecular Medicine, University of Kuopio; Departments of [2]Surgery, [3]Clinical Pathology, and [4]Gene Therapy Unit, Kuopio University Hospital, Kuopio, Finland; [5]Department of Biochemistry and Pharmacy, Åbo Akademi University, Turku, Finland; and [6]Academic Development Unit, University of Tampere, Tampere, Finland

Abstract

Oncolytic viruses are a promising tool for treatment of cancer. We studied an oncolytic Semliki Forest virus (SFV) vector, VA7, carrying the enhanced green fluorescent protein gene (*EGFP*), as a novel virotherapy candidate against unresectable osteosarcoma. The efficiency and characteristics of the VA7-EGFP treatment were compared with a widely studied oncolytic adenovirus, Ad5Δ24, both *in vitro* and *in vivo*. VA7-EGFP resulted in more rapid oncolysis and was more efficient at low multiplicities of infection (MOI) when compared with Ad5Δ24 *in vitro*. Yet, in MG-63 cells, a subpopulation resistant to the VA7-EGFP vector emerged. In subcutaneous human osteosarcoma xenografts in nude mice treatment with either vector reduced tumor size, whereas tumors in control mice expanded quickly. The VA7-EGFP–treated tumors were either completely abolished or regressed to pinpoint size. The efficacy of VA7-EGFP vector was studied also in an orthotopic osteosarcoma nude mouse model characterized by highly aggressive tumor growth. Treatment with oncolytic SFV extended survival of the animals significantly ($P < 0.01$), yet none of the animals were finally cured. Sera from SFV-treated mice contained neutralizing antibodies, and as nude mice are not able to establish IgG response, the result points out the role of IgM class antibodies in clearance of virus from peripheral tumors. Furthermore, biodistribution analysis at the survival end point verified the presence of virus in some of the brain samples, which is in line with previous studies demonstrating that IgG is required for clearance of SFV from central nervous system. [Cancer Res 2008;68(20):8342–50]

Introduction

Osteosarcoma is an aggressive malignant tumor primarily of children and young adults that is characterized by proliferation of malignant mesenchymal cells producing immature bone or osteoid (1, 2). It typically metastazises into lungs already at early phase (1). Development of preoperative (neoadjuvant) and postoperative (adjuvant) chemotherapy attacking the pulmonary micrometastases has dramatically improved prognosis of osteosarcoma patients during the last decades (2). Currently, long-term disease-free survival can be achieved in 60% to 70% of patients diagnosed with osteosarcoma (2). Despite the improvement in the survival rates, patients presenting with radiologically verified pulmonary metastases at the time of diagnosis, as well as patients with tumors at unresectable locations or with a recurrent disease, still have a poor prognosis and novel treatment modalities are urgently needed (1, 3).

Targeting tumors with oncolytic viruses is a promising approach for cancer treatment (4–7). These are modified or naturally oncotropic viruses, which selectively replicate in malignant tumor cells and finally destroy them via oncolysis (4). In this study, we used two distinct oncolytic viruses, an attenuated Semliki Forest virus (SFV) vector VA7-EGFP (8) and a conditionally replicating adenovirus Ad5Δ24 (9).

SFV is an enveloped positive-strand RNA-virus of the alphavirus genus. Wild-type SFV is a pathogen of small rodents and in mice infection with a "prototype" SFV strain L10 leads to fatal encephalitis (10). In humans, SFV is usually considered nonpathogenic; however, some reports indicate that the virus can cause human disease (11, 12).

SFVA7(74), an avirulent strain of SFV, carries several distinct attenuating mutations within the nonstructural open reading frame (13, 14). In addition, the VA7-EGFP vector contains a single amino acid change (Ile to Val) at position 11 of nsP3, which further reduces pathogenicity (14). The construction of the fluorescent marker gene EGFP carrying replication-competent VA7-EGFP vector has been previously described (8). In immunocompetent adult mice, infection with the SFVA7(74) strain and the derived oncolytic VA7-EGFP vector leads to transient replication in the central nervous system (CNS) but does not cause encephalitis (15). Also, in mice with severe combined immunodeficiency lacking acquired immune responses, replication of SFVA7(74) is restricted to small perivascular foci, although these mice are unable to clear the virus that finally leads to their death (16). However, in newborn mice with normal immune system, also SFVA7(74) causes fatal encephalitis (16). This is likely to be related to the greater susceptibility of the immature CNS to the SFV infection.

Adenoviruses are common human pathogens known to cause a variety of clinical pictures depending on the serotype in question (17). Adenovirus serotype 5 (Ad5) is extensively used for engineering the virus for therapeutic purposes. Wild-type Ad5 can cause acute febrile pharyngitis, pertussis-like syndrome, and hepatitis (17). In immunocompetent individuals, most adenovirus infections are asymptomatic or mild, but especially in immunocompromised patients, adenoviruses can cause severe or fatal disease (18).

Conditionally replicating adenoviruses (CRAd) are genetically engineered to replicate specifically in malignant cells with genetic defects not present in normal cells (19). Defects in p16/Rb/E2F

Requests for reprints: Anna Ketola, A. I. Virtanen Institute for Molecular Sciences, Department of Biotechnology and Molecular Medicine, University of Kuopio, P.O.B. 1627, FI-70211 Kuopio, Finland. Phone: 358-40-3553790; Fax: 358-17-163030; E-mail: anna.ketola@uku.fi.

doi:10.1158/0008-5472.CAN-08-0251

signaling pathway are related to the loss of cell cycle control in malignant cells and are commonly found in malignant tumors, including osteosarcomas (1). The conditionally replicating adenovirus Ad5Δ24 used in this study selectively replicates in tumors with alterations in p16/Rb/E2F pathway (9).

Aim of this study was to investigate the therapeutic utility of the oncolytic SFV vector VA7-EGFP against osteosarcoma using *in vitro* and *in vivo* models. The characteristics of this novel candidate for virotherapy of osteosarcoma were compared with a widely studied oncolytic adenovirus Ad5Δ24 (9). So far, the best results with both oncolytic viruses have been achieved using intratumoral route of administration. Therefore, we focused on intratumoral administration, which could be applicable for treatment of osteosarcoma tumors at unresectable locations.

Materials and Methods

Cell lines. We used four human osteosarcoma cell lines: U-2-OS (ATCC HTB-96), MG-63 (ATCC CRL-1427), Saos-2 (ATCC HTB-85), and Saos2LM7. The Saos2LM7 cell line was created by passaging Saos-2 cells several times through lungs of athymic mice to improve tumorigenicity in lungs (20–22). BHK-21 cells (ATCC CCL-10) and 293 cells (Microbix) were used for production and titration of VA7-EGFP vectors and CRAd, respectively. K7M3 mouse osteosarcoma cells (23) and Saos2LM7 cells, both used for animal models, were kind gifts from Dr. Chand Khanna (Pediatric Oncology Branch, Center for Cancer Research, National Cancer Institute, NIH, Bethesda, Maryland) and Dr. Eugenie Kleinerman (Children's Cancer Hospital, The University of Texas, M. D. Anderson Cancer Center, Houston, Texas). All cell lines were grown in DMEM (Cambrex), supplemented with 10% fetal bovine serum (FBS; Euroclone Ltd.) and 50 μg/mL gentamicin (Cambrex), at 37°C in the presence of 5% CO_2.

Vectors. Adenovirus vectors Ad5Δ24 (a kind gift from Dr. David Curiel, University of Birmingham, Alabama; ref. 9) and Ad5Δ24-TKGFP (24) were produced using standard techniques, and infective titers were determined using plaque assay. VA7-EGFP was produced as previously described (25). The vector-containing medium was collected and purified with a 0.2-μm pore size filter. Infective titer [transducing units (tu)/mL] for VA7-EGFP vector was determined with flow cytometry by measuring the number of EGFP-expressing cells 7 h posttransduction. Viruses were stored at −70°C. For *in vitro* experiments, we used a Ad5Δ24-TKGFP preparation stored in 10% glycerol containing 7.7×10^{10} plaque-forming unit (pfu)/mL and a VA7-EGFP preparation containing 1.0×10^9 tu/mL. For *in vivo* experiments, we used Ad5Δ24 preparation stored in 5% sucrose containing 1.84×10^{10} pfu/mL and VA7-EGFP preparation containing 3.5×10^9 tu/mL.

Vector spreading in cell cultures. Cells were seeded on 12-well plates 50,000 cells per well and transduced on the next day using different MOIs (Fig. 1). VA7-EGFP transductions were carried out in Optimem 1 with Glutamax 1-medium (Invitrogen) for 1 h in a 300-μL volume. Then 1.5 mL DMEM with 10% FBS was added onto each well. Ad5Δ24-TKGFP transductions were performed in DMEM with 2% FBS using 400 μL transduction volume overnight. Then 1 mL DMEM with 2% FBS was added and replaced with fresh DMEM with 2% FBS every other day. Cells were harvested or fixed with 4% paraformaldehyde at different time points for flow cytometry and fluorescence microscopy.

Oncolysis. Cells were transduced with VA7-EGFP and Ad5Δ24-TKGFP vectors as described above. DMEM with 4% FBS for adenovirus-transduced cells was added after transduction and replaced with fresh medium every other day. Cells were stained with crystal violet at different time points (Fig. 2).

Subcutaneous Saos2LM7 human osteosarcoma tumors. The cells were prepared for tumor induction as described previously (26). Sixteen 5-wk-old HsdCpb:NMRI-Foxn$^{nu/nu}$ nude mice (Harlan) received intracutaneous injections of 3×10^6 Saos2LM7 cells in volume of 50 μL into both flanks. Tumor volume was monitored twice a week as described previously (27). Because the tumorigenicity of the Saos2LM7 cells was below 100%, only the animals that developed bilateral progressively growing tumors were selected for the study. Treatment was started when tumors of the selected animals had average volume of ~13 mm^3. For each intratumoral injection, 30 μL undiluted virus preparation or 0.9% NaCl (for control group) was used per tumor (1.1×10^8 tu/tumor for VA7-EGFP and 5.5×10^8 pfu/tumor for Ad5Δ24-treated mice). Injections were repeated after 7 and 14 d. For tumor cell or virus injections, mice were anesthetized with s.c. fentanyl-fluanison-midazolam. Animals were sacrificed when the average tumor size in control group exceeded 150 mm^3. Preliminary studies showed that tumors growing beyond this size frequently ulcerated spontaneously. This end point was selected for ethical reasons and to exclude the possibility that infection and inflammation related to ulceration of control tumors would confuse the interpretation of histologic findings. Tumors were weighted and fixed in 4% paraformaldehyde for 24 h for histology.

Orthotopic K7M3 osteosarcoma tumor model. For tumor cell injections, 5-wk-old HsdCpb:NMRI-Foxn$^{nu/nu}$ nude mice (Harlan) were anesthetized, and K7M3 cells (1.2×10^6; ref. 22) in volume of 10 μL Optimem 1 with Glutamax 1 medium were injected axially into the proximal left tibia of mice with 27G 3/4" needle (TerumoNeolus) and a stopper allowing 4-mm penetration depth, according to technique developed by Berlin and colleagues (28) and later used by others (22). Ten μL suspension was injected, and after 10 s, the needle was removed. Temgesic (Reckitt Benckiser Healthcare Ltd.) 0.01 mg/mL, 30 μL per mouse, was administered s.c. to the animals for postoperative analgesia.

Tumor volume (V) was measured thrice per week (or daily when criteria for sacrificing animal were close to be fulfilled) as described previously (28). Treatment was started when average tumor volume was 13.4 mm^3. Thirty-microliter-volume of VA7-EGFP vector (1.05×10^8 tu) for treatment group (n = 8) or 0.9% NaCl for control group (n = 8) was injected into tumors. Injections were repeated weekly until the animals were sacrificed.

Survival end points were as follows: (*a*) weight decrease over 20% during experiment, (*b*) severe limb swelling (circumference of tumor bearing left hind limb >1.5 times that of right hind limb), (*c*) tumor volume exceeding 125 mm^3, or (*d*) total inability to use tumor bearing limb. These criteria for sacrificing the animals were in line with the national animal welfare guidelines. Animals were sacrificed with CO_2. Lungs and left tibial bones with the tumor mass as well as surrounding tissues were necropsied for histology and fixed for 24 h with 4% or for 48 h with 10% paraformaldehyde in PBS, respectively. Part of the tumor, the brains, serum, and peripheral organs including liver, kidney, heart, and spleen were sampled and stored in −70°C. Sera and tissue homogenates were analyzed for presence of virus with a plaque titration assay.

Noninvasive *in vivo* imaging. For magnetic resonance imaging (MRI), lower limbs of mice were fixed in caudally extended position. MRI was carried out in a 4.7 T magnet (Magnex Scientific Ltd.) equipped with a 170 mT/m gradient set interfaced to a Varian ^{UNITY}*INOVA* console (Varian, Inc.). A half-volume surface coil (High Field Imaging) was used for transmission and receiving of the MR signal. Fifteen 1-mm-thick slices with 256 points in free induction decay and 128 phase encoding steps in field of view 2.5×2.5 cm^2 was imaged using T2-weighted multislice spin echo sequence (repetition time, 2,500 ms; echo time, 70 ms).

Computed tomography was used for imaging of lungs. Computed tomography (CT) projection images with matrix size 1,120 × 1,184 (X-ray tube voltage 60 kV and tube current 425 μA) were acquired using the Flex X-O small animal imaging system (Gamma Medica, Inc.). For CT image reconstruction, Exxim reconstruction software (Exxim Computing Corporation) was used with 512 × 512 × 512 final matrix size and pixel resolution of 170 μm for all three spatial directions.

Histology. Bone containing samples were decalcified for 10 to 12 d in decalcification solution consisting of 10% EDTA and 4% formaldehyde in 0.1 mol/L phosphate buffer that was replaced with fresh solution every other day. The samples were dehydrated and embedded in paraffin, cut into 4-μm sections, and stained with H&E. For immunostaining, we used either rabbit polyclonal anti-SFV antibody (1:2,500) or rabbit polyclonal anti-Ad2 E1A antibody (1:750; recognizes also Ad5 E1A antigen; Santa Cruz Biotechnology, Inc.) coupled with a peroxidase anti-rabbit antibody conjugate (Vectastain ABC kit; Vector Laboratories, Inc.).

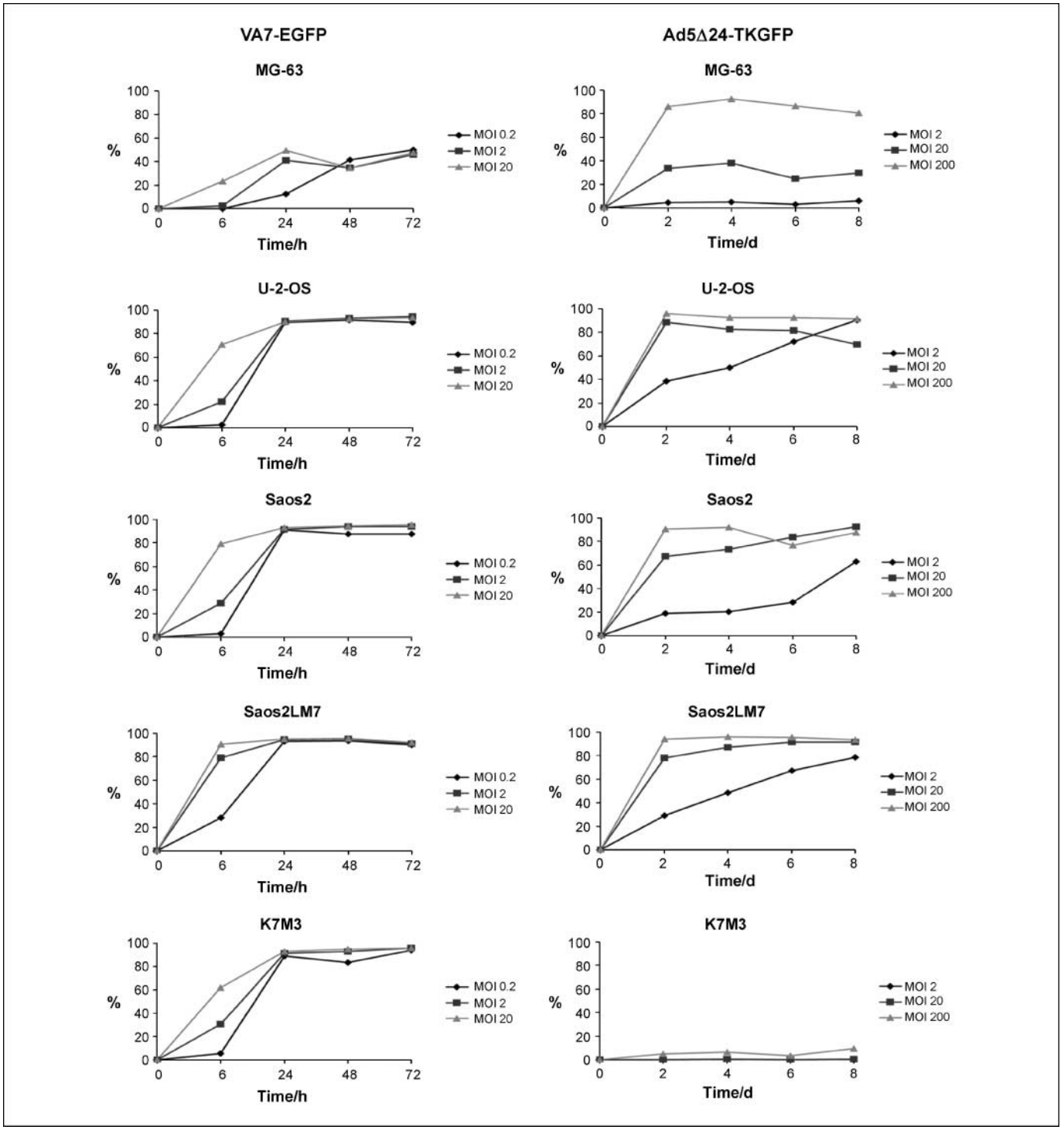

Figure 1. Propagation of VA7-EGFP and Ad5Δ24-TKGFP vectors in osteosarcoma cell cultures at different time points posttransduction. Proportion of marker gene–expressing cells (%) was detected with flow cytometry. A dose response pattern was clearly visible 6 h after transduction with VA7-EGFP. In four of the five osteosarcoma cell lines studied, the proportion of EGFP marker gene–expressing cells reached almost 100% in 24 h with all used MOIs and stayed high at all time points. However, one of the human osteosarcoma cell lines, MG-63, seemed to be relatively resistant to VA7-EGFP infection. Ad5Δ24-TKGFP carrying the TKGFP suicide-marker fusion gene was used to show Ad5Δ24 propagation in osteosarcoma cell cultures. Vector propagation was observed in three of five osteosarcoma cell lines studied. MG-63 cells were effectively transduced with Ad5Δ24-TKGFP at high MOI but were not permissive for efficient propagation of the vector. Additionally, K7M3 mouse osteosarcoma cells were highly resistant to both transduction with and propagation of Ad5Δ24-TKGFP.

Detection of neutralizing antibodies. Serum samples collected from animals at the end point of the survival study were analyzed for presence of neutralizing antibodies. K7M3 mouse osteosarcoma cells were split onto 48-well plates, 3×10^4 cells per well. On the next day, VA7-EGFP vector was mixed with different serum dilutions, incubated at +37°C for 1 h, and then added onto cells. Transductions were carried out with MOI 0.1 in presence of 1:20, 1:100, 1:500, or 1:2,500 serum. All samples were analyzed in triplicates. Cells were harvested at 24-h time point, and the proportion

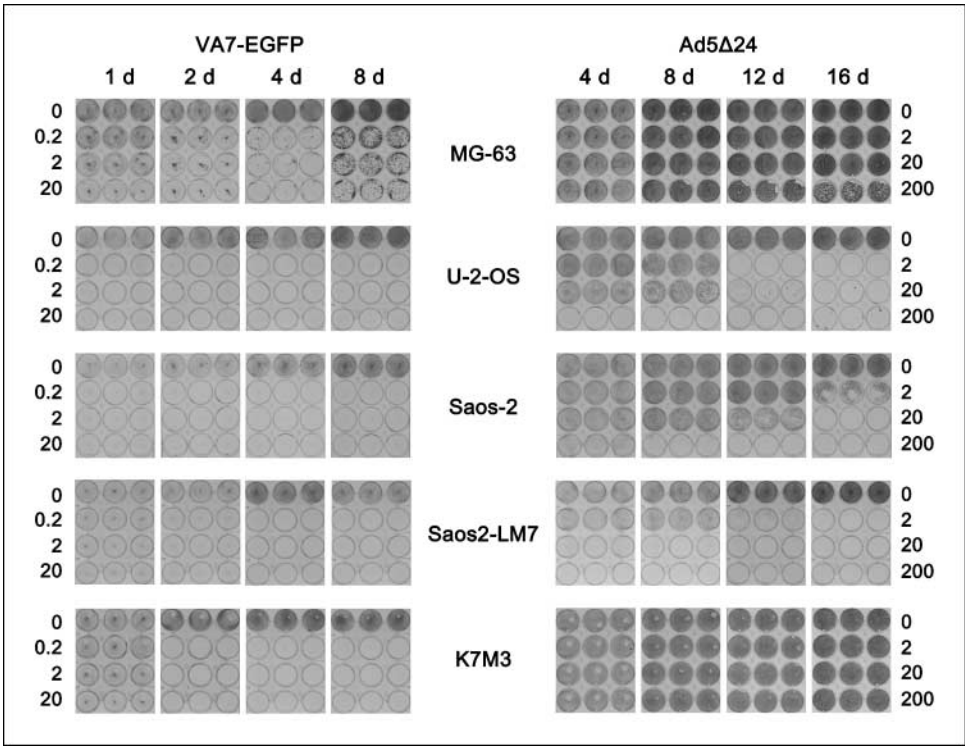

Figure 2. Oncolysis in osteosarcoma cell cultures after infection with VA7-EGFP or Ad5Δ24 vectors. Crystal violet staining of viable cells at different time points was used for detection of cell destruction. Propagation of VA7-EGFP was very rapid, resulting in extensive oncolysis only 1 d after infection in 2 of 5 cell lines studied (U-2-OS and Saos-2), and after 2 d, massive cell death was observed in all cultured cell lines. However, in MG-63 cells, a subpopulation resistant to VA7-EGFP rapidly emerged. Ad5Δ24 efficiently destroyed three of five studied osteosarcoma cell lines. In U-2-OS and Saos2-LM7 cells MOI 2 was sufficient to induce complete oncolysis by day 12. In Saos-2 cells, MOI 20 was needed for efficient cell destruction by day 16. Still, two of the five cell lines (K7M3 and MG-63) seemed to be highly resistant to adenovirus-mediated oncolysis.

of EGFP-expressing cells was determined with flow cytometry. Cells transduced with VA7-EGFP virus preincubated with rabbit anti-SFV serum were used as a positive control. Cells transduced with VA7-EGFP without serum pretreatment or preincubated with serum from 0.9% NaCl–treated control animals functioned as negative controls.

Statistical analyses. GraphPad Prism 3.0 (GraphPad Software, Inc.) was used for statistical analyses. For comparison of tumor volumes and tumor weights, the two-way ANOVA and one-way ANOVA were used, respectively, both with Bonferroni's multiple comparison test. For analysis of survival data the log-rank test was used. P value of <0.01 was considered as statistically significant.

Results

Propagation and oncolysis *in vitro*. Propagation of two oncolytic viruses, SFV VA7-EGFP and conditionally replicating adenovirus Ad5Δ24-TKGFP carrying the *TKGFP* suicide-marker fusion gene (herpes simplex type 1 thymidine kinase-green fluorescent protein; refs. 24, 29) was studied in osteosarcoma cells *in vitro* (Fig. 1). VA7-EGFP efficiently propagated in four of five studied cell lines. In MG-63 cells, however, its propagation was moderately restricted.

Compared with the rapid spreading of infection with SFV, Ad5Δ24-TKGFP required more time and higher MOI to spread throughout the cell culture. MG-63 cells were effectively transduced with Ad5Δ24-TKGFP with high MOIs, but virus propagation was severely restricted. Also, the K7M3 mouse osteosarcoma cells were highly resistant to both transduction with and propagation of the oncolytic adenovirus vector. This was not unexpected because most rodent cell types are considered nonpermissive for adenovirus replication (30–32).

Extent of viral oncolysis and propagation kinetics were investigated in osteosarcoma cell cultures infected with VA7-EGFP or Ad5Δ24 using crystal violet assay (Fig. 2). VA7-EGFP caused extensive cell death in all tumor lines studied. However, in MG-63 cells emergence of a resistant cell population was evident and despite initial decline, these cells continued to divide in the presence of virus (see 8-day time point in Fig. 2).

Kinetics of adenovirus infection was much slower compared with SFV and higher amounts of virus were needed for complete lysis of the cultured osteosarcoma cells. Ad5Δ24 effectively destroyed three of five studied cell lines. MG-63 and K7M3 cells were highly resistant to adenoviral oncolysis. Yet, with K7M3 cells, this result was expectable (see above).

Characterization of the Saos2LM7 subcutaneous osteosarcoma mouse model. Nine of the 16 mice developed tumors on both flanks. Two mice developed well-growing and viable-looking tumor on only one flank, whereas tumors on the other flank spontaneously regressed. One of 16 mice showed spontaneous complete healing of both tumors. Because the tumorigenicity of the Saos2LM7 cells was below 100%, only those mice with bilateral progressively growing tumors were accepted for study evaluating the efficiency of SFV virotherapy.

Therapeutic effect in subcutaneous Saos2LM7 tumors. Statistically significant difference in tumor size compared with controls was achieved already 11 days after starting the treatment with both SFV ($P < 0.001$, ***) and adenovirus ($P < 0.01$, **; Fig. 3*A*). The mice were sacrificed 3 weeks after the first injection. At the end point, both oncolytic viruses yielded statistically significant reduction in tumor volume ($P < 0.001$, ***; Fig. 3*A*) and in tumor weight ($P < 0.001$, ***; Fig. 3*B*) compared with controls. The photograph taken at the time of sacrifice clearly shows the therapeutic effect (Fig. 3*C*). All tumors were sampled for histology with the exception of one of six SFV-treated tumors that seemed completely cured and therefore could not be identified for sampling.

Histopathologic analysis of the subcutaneous Saos2LM7 tumors was performed with H&E-stained sections (Fig. 3*D, top row*), and the presence of virus in tumors was verified with immunostaining

(Fig. 3*D, bottom row*). In saline-treated control tumors, the malignant cells showed high number of mitoses and apoptotic cells, indicating high proliferative activity. In tumors treated with the VA7-EGFP or Ad5Δ24 vectors, reactive fibrosis and calcification were detected. In VA7-EGFP–treated tumors, only few tumor cells were left, surrounded by reactive fibrosis. In addition, large areas of cell debris were seen as remnant from SFV-mediated oncolysis. In one of the SFV-treated tumors, no malignant cells could be identified in microscopy of the H&E-stained samples.

Immunohistochemical staining with antiadenovirus and anti-SFV antibodies verified the presence of virus in all treated tumors. In tumors treated with Ad5Δ24, virus-positive cell areas of variable size were seen inside the tumor tissue. In addition, single virus–positive cells were detected. In SFV-treated tumors, the positively stained cells were lining areas of complete cell destruction, which were surrounded by fibrosis. The remaining few clusters of SFV-negative tumor cells were surrounded by fibrosis, possibly protecting the tumor cells from oncolytic SFV infection.

Characterization of the K7M3 orthotopic osteosarcoma mouse model. For further evaluation of oncolytic SFV, we established an orthotopic mouse model of osteosarcoma. Tumorigenicity of K7M3 cells in 5-week-old HsdCpb:NMRI-Foxn$^{nu/nu}$ nude mice was 100%. In 80% of mice, visible tumor nodule could be identified on the proximal end of the tibia 16 days post tumor inoculum, whereas in some mice, development of a visible tumor was delayed up to several weeks. In these mice, the tumors were located under the muscles of the leg or the tumor growth was taking place merely inside the medullar cavity and visible tumor developed only after invasion through the cortical bone. A large proportion of the mice developed gross edema, eventually leading to inability to use the limb. Tumors grew aggressively and average survival of the untreated mice according to above-mentioned criteria was <1 month.

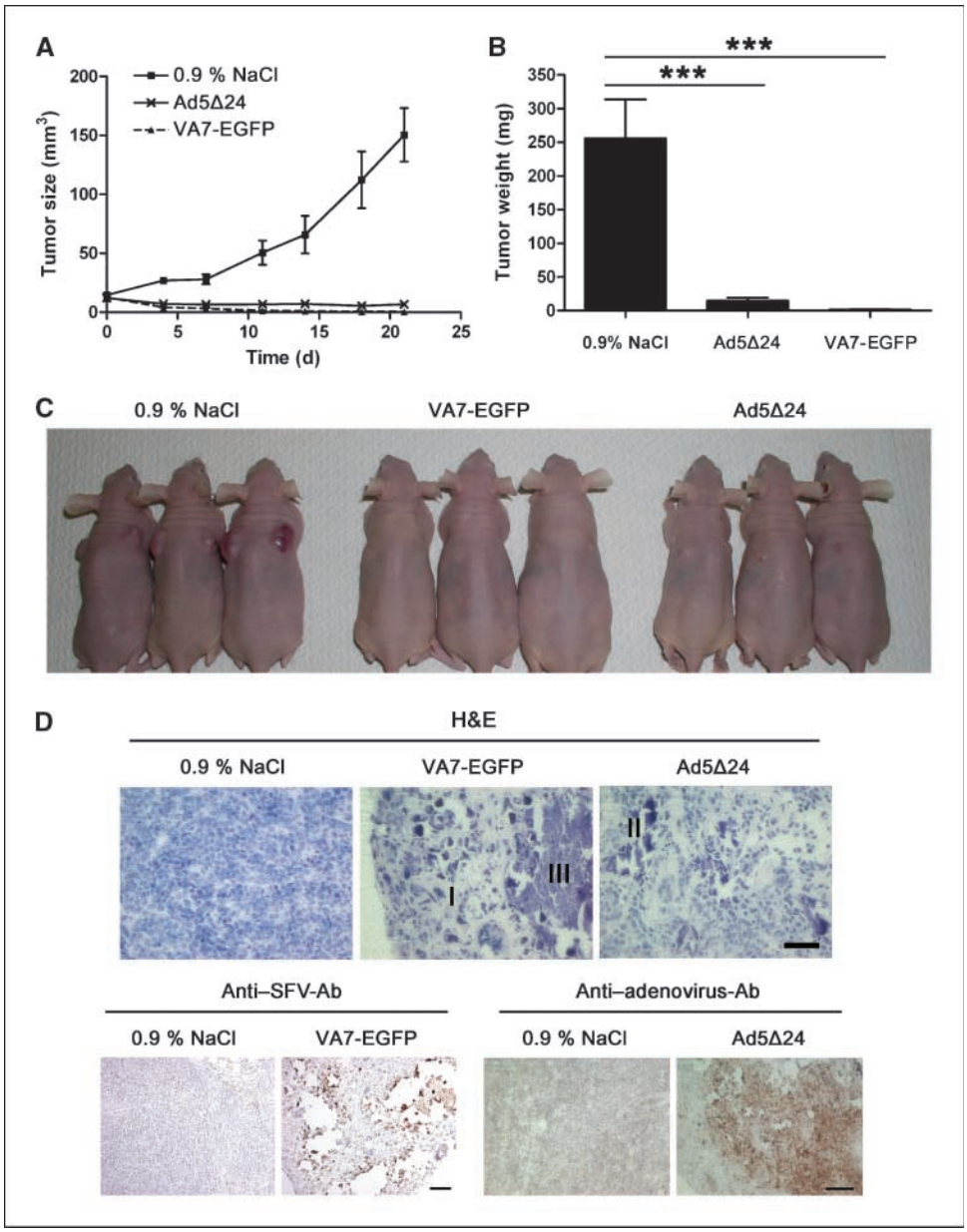

Figure 3. Therapeutic effect of both VA7-EGFP and Ad5Δ24 viruses was tested in subcutaneous Saos2LM7 human osteosarcoma tumors implanted into nude mice. The mice received intratumoral injections of virus or 0.9% NaCl weekly for 3 wk. Significant reduction in tumor volume was observed in the treatment groups compared with controls from day 11 as determined using Bonferroni's multiple comparison test (*A*). At the time of sacrifice on day 21, significant difference was observed in tumor weight between the SFV- or adenovirus-treated groups and negative controls ($P < 0.001$, one-way ANOVA; *B*). Photograph illustrating the therapeutic effect of oncolytic VA7-EGFP and Ad5Δ24 viruses on mice day 21 post treatment compared with controls that received 0.9% NaCl (*C*). Tumors were sampled for histology (*D*). In contrast to control tumors treated with 0.9% NaCl, tumors treated either with VA7-EGFP or Ad5Δ24 showed marked fibrosis (*I*) and reactive calcifications (*II*). In SFV-treated tumors, large necrotic areas were found (*III*). Immunostaining with anti-SFV antibody or anti-adenovirus antibody showed brown-colored virus-positive areas, whereas the 0.9% NaCl-treated control tumors remained negative. *Scale bars*, 100 μm in H&E stainings and 200 μm in immunostainings.

We used noninvasive MRI and CT imaging for characterization of features of the orthotopic K7M3 tumor model. In T2-weighted MRI, the tumor mass was detected as irregularly increased or decreased signal corresponding to the location of the visible tumor mass, a pattern often found also in clinical setting (33). However, T2-weighted MRI revealed also grossly enlarged blood vessels and edema (seen as increased signal in MRI) in the lower limb muscles (Fig. 4*A, right*).

With CT imaging, macroscopic metastases with diameter of at least 1.5 mm could be clearly visualized in the peripheral lung (Fig. 4*B*). However, reliable detection of small metastases located around the hilus area was complicated by the vascular structures. Only few animals developed large pulmonary nodules before meeting the euthanasia criteria. Most metastases remained microscopic or smaller than 1 mm at the time of sacrifice.

Tumors and their surrounding tissues were sampled together and processed for histology followed by H&E staining. Microscopic analysis showed high number of mitotic cells and aggressive invasion of tumor into the surrounding tissues (Fig. 4*C*) including bone, bone marrow, muscle, and cartilage. Lungs of the tumor-bearing mice were also sampled for histology both during the preliminary experiment and the survival study (next chapter). Microscopy of H&E-stained lung sections showed that primary tumors implanted into the tibial bone were capable of metastasizing into the lungs, which is an important feature of osteosarcoma in clinical setting (Fig. 4*D*; ref. 1). Metastases were frequently located in close vicinity of blood vessels and sometimes even growing inside the vascular lumen. This indicates hematogenous spreading of tumor cells into the lungs, which is comparable with the clinical picture of osteosarcoma (3).

Improved survival in orthotopic K7M3 tumor model. Treatment with intratumoral injections of VA7-EGFP weekly significantly improved the survival in the orthotopic osteosarcoma model, compared with the control group that received 0.9% NaCl injections ($P = 0.0017$; Fig. 5*A*). However, none of the mice was eventually cured. To investigate the reasons for the treatment failure, serum of the sacrificed animals was analyzed for its capacity to neutralize the virus. Complete inhibition of infection with VA7-EGFP MOI 0.1 was observed with 1:20 serum dilution, and with 1:100 to 1:2,500 dilutions, the infection was clearly suppressed compared with controls (Fig. 5*B*).

Immunostaining with anti–SFV-Ab confirmed the clearance of VA7-EGFP from tumors at the survival end point. Most of the tumor samples from the treatment group were negative for SFV antigens. In some samples, a few single SFV-positive cells could be found (Fig. 5*C*). Furthermore, VA7-EGFP was not found from pulmonary metastases or from the surrounding healthy lung by anti–SFV-Ab immunostaining at the survival end point (data not shown).

We also studied the biodistribution of VA7-EGFP at the survival end point (Fig. 5*D*) and could verify the almost complete clearance of the virus from tumors with residual of 7.6×10^3 pfu/g or less. Three of eight tumors and all serum samples remained negative for virus. Furthermore, analysis of other peripheral tissues revealed only low amounts of virus in cardiac muscle and spleen of some animals, whereas liver and kidney remained completely negative for SFV. However, in 5 brain samples out of 8 from the SFV-treated mice, the virus was detected, highest titer being 7.2×10^5 pfu/g, indicating that the virus could replicate to some extent in the brain tissue of some of the animals. Still, none of the mice showed neurologic symptoms during the study.

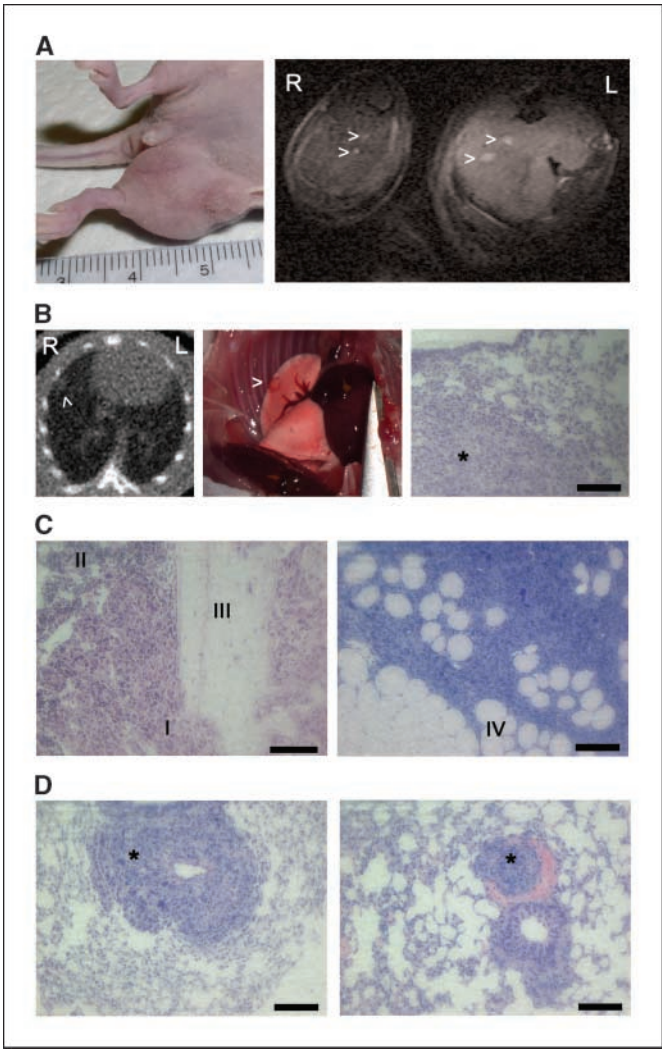

Figure 4. K7M3 osteosarcoma cells were implanted into the left proximal tibia of nude mice to induce orthotopic tumors (*A, left*). Gross edema was detected with T2-weighted nuclear magnetic resonance imaging as increased signal and dilation of blood vessels (*arrowheads*) in tumor-bearing left (*L*) hind limb (*A, right*). Lung metastasis imaged with CT (*B, left, arrowhead*) was confirmed in sacrificed animal: a metastatic tumor nodus was found at corresponding location (*B, middle, arrowhead*). The finding was also confirmed by histologic sampling (*B, right*; *, metastasis). Histopathologic analysis of the primary tumor (*C*) showed aggressive tumor growth and invasion of the malignant cells (*I*) into the surrounding bone marrow (*II*), bone (*III*), and muscle (*IV*). K7M3 tumors growing in the proximal tibia were also capable of sending metastases (*) into the lungs of mice (*D, left*). The micrometastases (*) were usually located in the near vicinity of the blood vessels. Vascular invasion was also found in some slides (*D, right*). The scale bars in figures correspond to 100 μm.

Discussion

Vector spreading and oncolysis in osteosarcoma cell cultures. The oncolytic adenovirus and SFV were tested for their capacity to infect, spread, and cause oncolysis in four human osteosarcoma cell lines, which differed from each other by their genetic profiles. As a common denominator, Saos-2, U-2-OS, and MG-63 cells all have some type of inactivation of the p16/Rb/E2F pathway (34). Our results are consistent with the statement that replication of the Ad5Δ24 is dependent on defective p16/Rb/E2F pathway (9): Ad5Δ24 could effectively replicate in both Saos-2 and U-2-OS cells. Efficient adenoviral replication and oncolysis took place in Saos2LM7 cells that presumably also are Rb defective,

similar to the parental cell line Saos-2. Interestingly, in MG-63 cells infected by Ad5Δ24, viral replication, and consequently, also oncolysis were severely restricted despite defective p16. A likely explanation for this is the low expression of coxsackie-adenovirus receptor (CAR), the primary receptor for Ad5 (35, 36). It has been shown that retargeting of Ad5Δ24 using an Arg-Gly-Asp motif (RGD-4C) toward integrins dramatically improves its oncolytic effect in MG-63 cells (37). In addition to retargeting via RGD-4C motif, the virus used by Witlox and colleagues (38) contained E3 region of the adenovirus genome deleted from the Ad5Δ24 used in this study. The E3 region has been found to potentiate the oncolytic efficacy of CRAd.

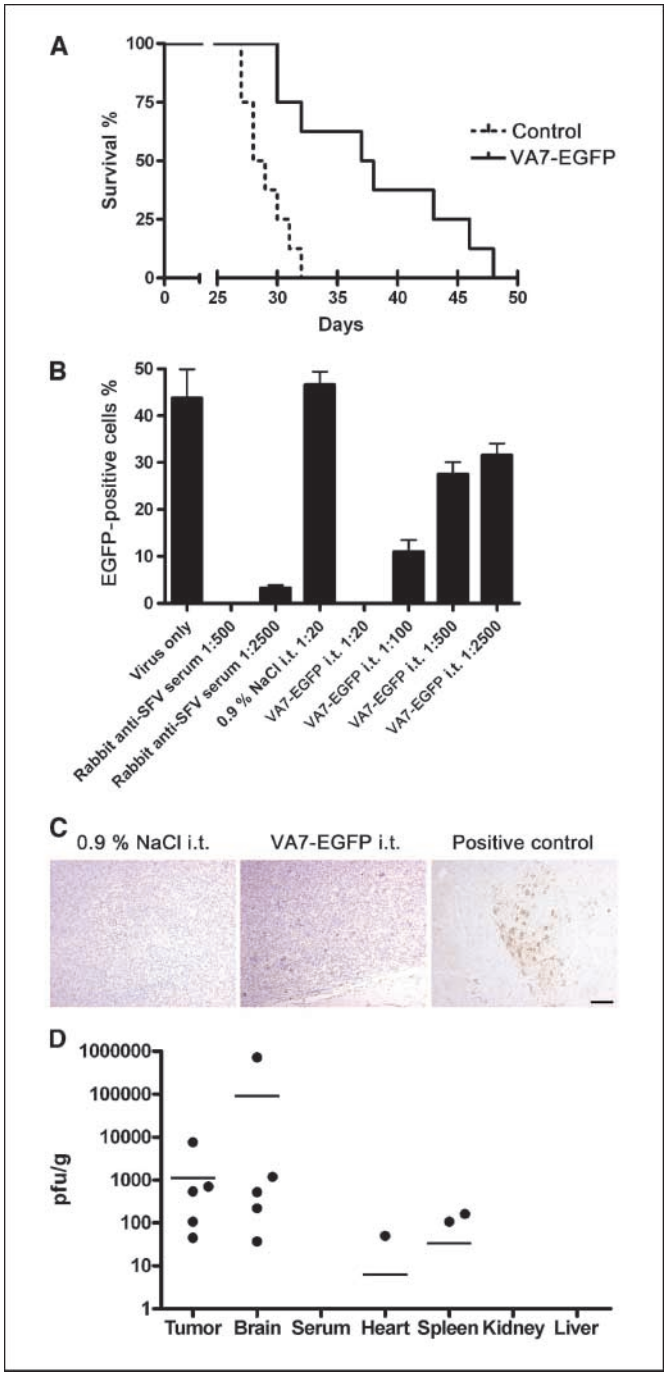

Figure 5. Treatment with oncolytic VA7-EGFP vector weekly significantly improved survival of mice bearing orthotopic K7M3 tumors ($P > 0.01$; *A*). Serum samples were collected from animals at the time of sacrifice. Capacity of serum dilutions to neutralize VA7-EGFP virus was studied with K7M3 cells *in vitro*. Rabbit anti-SFV serum was used as positive control for antibody-induced inhibition of infection. Untreated VA7-EGFP virus and VA7-EGFP preincubated with serum from mice that received 0.9% NaCl were used as negative controls (*B*). Immunostaining of histologic tumor samples with anti-SFV antibody confirmed the clearance of oncolytic SFV from tumors at survival end point (*C*). Brain tissue of SFV-infected mouse was used as a positive control. Biodistribution of VA7-EGFP was analyzed at the survival end point (*D*).

Transduction and replication of VA7-EGFP was moderately impaired only in MG-63 cells of all analyzed cell lines. Interestingly, a subpopulation of resistant cells rapidly emerged in this cell line upon viral presence. Reduced efficacy of transduction and limited oncolysis are likely to be related to the vigorous type I IFN response, and subsequent accumulation of MxA observed in these cells as a response to alphavirus infection.[7] This hypothesis is supported by the fact that similar pattern of rapid emergence of resistant cell population was observed in A549 lung carcinoma cells infected with the VA7-EGFP (39). A549 cells display a robust type I IFN response and strong MxA expression against SFV infection (40). The type I IFN response and the MxA protein itself have been found to inhibit SFV infection both *in vitro* and *in vivo* (41, 42–45).

In clinical setting, the osteosarcoma tumors have been found to consist of different subpopulations of tumor cells with variation in their histologic features (46) and genetic profiles (47). The selection and outgrowth of resistant cell populations in the presence of the oncolytic VA7-EGFP vector indicate that development of resistance might be a problem in a clinical setting. Therefore, in the future, the efficacy of oncolytic SFV virotherapy should be assessed in combination with other therapeutic strategies, including chemotherapeutic agents currently used against osteosarcoma.

Therapeutic effect in subcutaneous Saos2LM7 tumors. One of the main factors contributing to the therapeutic efficacy of Ad5Δ24 is the expression of CAR, the primary receptor for Ad5 on the target cells. Saos-2 cells have been shown to express CAR (48), and our *in vitro* experiments showed that the derived Saos2LM7 cell line was at least as sensitive for Ad5Δ24-mediated transduction and oncolysis as the parental Saos-2. Therefore, good response to Ad5Δ24 treatment in Saos2LM7 tumor model was predictable. However, previous report by Witlox and colleagues (48) described low levels of CAR expression in several primary osteosarcoma tumor samples. Because the expression of CAR has been found to be a critical determinate for the efficacy of oncolysis exerted by CRAd (35), the low CAR expression can potentially limit the utility of Ad5Δ24 against osteosarcoma. Attempts to circumvent this problem have been made. Witlox and colleagues (37) showed that a conditionally replicating adenovirus, retargeted toward integrins, showed improved oncolysis in most osteosarcoma cell lines and in a panel of primary OS cell cultures. Still, in Saos-2 cells no further improvement was achieved with this type of retargeting.

Treatment with oncolytic SFV was found to be highly efficient against Saos2LM7 tumors. One characteristic of Saos2LM7 cells that makes them remarkably sensitive for oncolytic SFV could be their defective innate immune response. We studied here the MxA response to infection with VA7-EGFP in Saos2LM7 cells with a method previously described by Rautsi and colleagues (40). No accumulation of MxA was observed (data not shown). In cells with intact innate immune responses, MxA is induced when cells are exposed to type I IFNs. MxA expression is strictly under regulation

[7] Unpublished data.

of the type I IFNs and can be used as a marker for type I IFN response (40).

Extended survival in orthotopic K7M3 tumor model by VA7-EGFP virotherapy. The highly aggressive growth of orthotopic K7M3 tumors, invasion to surrounding tissues, and emergence of hematogenous pulmonary metastases make this tumor model comparable with the clinical picture of human osteosarcoma. Additionally, T2-weighted MRI revealed grossly enlarged blood vessels and edema in the lower limb muscles (Fig. 4*A, right*). K7M2, the parental cell line of K7M3, was found to express vascular endothelial growth factor (VEGF). The K7M2 tumors were characterized with increased angiogenic potential. Both structurally normal and ill-formed blood vessels were present throughout the tumors. The K7M2 pulmonary metastases (from which the K7M3 cells were derived) showed even greater vascularity compared with respective primary tumors (49). A robust VEGF expression is also related to increased vascular permeability and tissue edema (50). Despite the aggressiveness of K7M3 tumors, treatment with the oncolytic VA7-EGFP vector led to significant improvement in survival compared with untreated controls. The intratumoral VA7-EGFP injections could potentially be applicable for treatment of primary tumors at unresectable locations or improving the quality of surgical margins after suboptimal resection of tumors arising for example in the pelvic area. The option to insert immunomodulatory transgenes into the VA7 vector to augment immune responses against tumor cells holds promise for improved efficacy especially against metastases. Therefore, further efforts for optimizing SFV virotherapy against osteosarcoma are warranted.

The biodistribution analysis of VA7-EGFP at the survival end point indicated asymptomatic CNS infection in some of the treated mice. These results obtained in immunocompromised nude mouse model are consistent with previously published studies (16, 25). The SFVA7(74) infection of athymic *nu/nu* nude mice has been reported to lead to transient viremia and persistent (>210 days) subclinical CNS infection (16). However, immunocompetent adult mice were able to clear the virus both from blood and CNS (16).

Factors potentially leading to treatment failure. It has been previously shown that emergence of resistant tumor cells can lead to eventual failure of VA7-EGFP therapy (15). In MG-63 cell cultures, a resistant subpopulation emerged during VA7-EGFP treatment, indicating that this may occur in osteosarcoma as well. Additionally, sera collected from SFV-treated mice were able to completely inhibit transduction and spreading of the VA7-EGFP vector in K7M3 cell cultures indicating presence of neutralizing antibodies, whereas sera from untreated mice showed no inhibition. A recent study by Määttä and colleagues (41) evaluating the therapeutic efficacy of oncolytic SFVA7(74) in syngeneic orthotopic rat glioma model reported only a limited antitumor activity due to emergence of IgG antibodies against SFV (25). Although IgM antibodies can clear the viremia during SFV infection, IgG antibodies are required for clearance of CNS infection (16). Unlike immunocompetent animals, nude mice are IgG deficient and IgM is the predominant class of antibodies (16).

Interestingly, in Saos2LM7 tumors VA7-EGFP virus was still present 3 weeks after the first injection. The virus was found in refractory tumor cells lining localized areas of tumor cell debris, surrounded by fibrous walls. The fibrous walls have been previously shown to protect uninfected tumor cells against VA7-EGFP infection (15). We hypothesize that the fibrous walls could also protect the oncolytic virus against attacks of the immune system, especially IgM-mediated inactivation. Another possible explanation for the better therapeutic response observed in Saos2LM7 model compared with K7M3 model is the enhancement of pre-existing immune responses against Saos2LM7 cells by VA7-EGFP infection. Unlike with K7M3 cells, the tumorigenicity of Saos2LM7 cells is below 100%, most likely due to partial rejection of the tumor by the immune system. Despite the lack of functional T cells, the other cells of the immune system, such as natural killer cells, may cause rejection of transplanted tumors in nude mice.

The available data suggests that vast majority of European population does not have pre-existing antibodies to SFV (51). Seroprevalence of this Old World alphavirus is more common in Africa (up to 37% rate found in Angola; refs. 52, 53). Still, the pre-existing antibodies are not so extensive problem with VA7-EGFP as with oncolytic adenoviruses. However, our present study shows the capacity of IgM response to stop SFV infection and inhibit oncolysis of peripheral tumors. These findings are likely to be significant for predicting potential hurdles of SFV virotherapy in clinical setting.

As a conclusion, this study shows the ability of oncolytic VA7-EGFP vector to effectively and specifically destroy osteosarcoma cells both *in vitro* and *in vivo*. The oncolytic effect of the VA7-EGFP and a conditionally replicative adenovirus Ad5Δ24 was studied in several human osteosarcoma cell lines. The *in vitro* studies showed a highly effective killing of malignant cells by oncolytic SFV. Compared with Ad5Δ24, VA7-EGFP vector showed more rapid and effective oncolysis with lower MOIs. Both oncolytic viruses were highly effective in subcutaneous human xenograft tumors, VA7-EGFP showing slightly more potent antitumor effect when compared with Ad5Δ24. Furthermore, VA7-EGFP vector significantly improved the survival of animals compared with controls ($P < 0.01$) in orthotopic osteosarcoma model. Our experimentation revealed also some potential hurdles for effective SFV virotherapy against osteosarcoma. In one of the cell lines studied, a resistant subpopulation of cells emerged in presence of VA7-EGFP. This observation warrants evaluation of combination therapies involving SFV and e.g., chemotherapeutic drugs used against osteosarcoma. Furthermore, our previous study in syngeneic rat glioma model showed the potency of IgG response to abolish the viral oncolysis in intracranial tumors (25). In the current study, emergence of anti-SFV IgM antibodies was found to be important in shutting down the oncolysis in peripheral tumors. One of the issues of special interest is the interaction of the immune system with therapeutic viruses. The innate and acquired immune responses have a fundamental effect in the efficiency and safety of oncolytic virotherapy. For improved therapeutic efficacy, arming the oncolytic VA7 vector with therapeutic or immunomodulatory transgenes is of great interest and warrants further studies.

Disclosure of Potential Conflicts of Interest

No potential conflicts of interest were disclosed.

Acknowledgments

Received 1/21/2008; revised 5/26/2008; accepted 7/15/2008.

Grant support: Finnish Medical Foundation and the North-Savo Regional Fund of the Finnish Cultural Foundation (A. Ketola), the K. Albin Johansson Foundation, and the Understödsförening Liv och Hälsa (A. Hinkkanen).

The costs of publication of this article were defrayed in part by the payment of page charges. This article must therefore be hereby marked *advertisement* in accordance with 18 U.S.C. Section 1734 solely to indicate this fact.

We thank A. Närvänen for help with CT imaging software; S. Juutinen, T. Kuusinen, and A. Laitinen for their skilful technical assistance; and E. Kleinerman, C. Khanna, C. Densmore, N. Koshkina, and S-F. Jia for providing cell lines.

References

1. Marina N, Gebhardt M, Teot L, Gorlick R. Biology and therapeutic advances for pediatric osteosarcoma. Oncologist 2004;9:422–41.
2. Carrle D, Bielack SS. Current strategies of chemotherapy in osteosarcoma. Int Orthop 2006;30:445–51.
3. Kansara M, Thomas DM. Molecular pathogenesis of osteosarcoma. DNA Cell Biol 2007;26:1–18.
4. Everts B, van der Poel HG. Replication-selective oncolytic viruses in the treatment of cancer. Cancer Gene Ther 2005;12:141–61.
5. Kirn D, Martuza RL, Zwiebel J. Replication-selective virotherapy for cancer: biological principles, risk management and future directions. Nat Med 2001;7:781–7.
6. Russell SJ. RNA viruses as virotherapy agents. Cancer Gene Ther 2002;9:961–6.
7. Vähä-Koskela MJ, Heikkilä JE, Hinkkanen AE. Oncolytic viruses in cancer therapy. Cancer Lett 2007;254:178–216.
8. Vähä-Koskela MJ, Tuittila MT, Nygårdas PT, et al. A novel neurotropic expression vector based on the avirulent A7(74) strain of Semliki Forest virus. J Neurovirol 2003;9:1–15.
9. Fueyo J, Gomez-Manzano C, Alemany R, et al. A mutant oncolytic adenovirus targeting the Rb pathway produces anti-glioma effect *in vivo*. Oncogene 2000;19:2–12.
10. Barrett PN, Sheahan BJ, Atkins GJ. Isolation and preliminary characterization of Semliki Forest virus mutants with altered virulence. J Gen Virol 1980;49:141–7.
11. Mathiot CC, Grimaud G, Garry P, et al. An outbreak of human Semliki Forest virus infections in Central African Republic. Am J Trop Med Hyg 1990;42:386–93.
12. Willems WR, Kaluza G, Boschek CB, et al. Semliki forest virus: cause of a fatal case of human encephalitis. Science 1979;203:1127–9.
13. Tuittila MT, Santagati MG, Röyttä M, Määttä JA, Hinkkanen AE. Replicase complex genes of Semliki Forest virus confer lethal neurovirulence. J Virol 2000;74:4579–89.
14. Tuittila M, Hinkkanen AE. Amino acid mutations in the replicase protein nsP3 of Semliki Forest virus cumulatively affect neurovirulence. J Gen Virol 2003;84:1525–33.
15. Vähä-Koskela MJ, Kallio JP, Jansson LC, et al. Oncolytic capacity of attenuated replicative Semliki Forest virus in human melanoma xenografts in severe combined immunodeficient mice. Cancer Res 2006;66:7185–94.
16. Amor S, Scallan MF, Morris MM, Dyson H, Fazakerley JK. Role of immune responses in protection and pathogenesis during Semliki Forest virus encephalitis. J Gen Virol 1996;77:281–91.
17. Jones MS II, Harrach B, Ganac RD, et al. New adenovirus species found in a patient presenting with gastroenteritis. J Virol 2007;81:5978–84.
18. Jogler C, Hoffmann D, Theegarten D, Grünwald T, Uberla K, Wildner O. Replication properties of human adenovirus *in vivo* and in cultures of primary cells from different animal species. J Virol 2006;80:3549–58.
19. Kirn D. Replication-selective oncolytic adenoviruses: virotherapy aimed at genetic targets in cancer. Oncogene 2000;19:6660–9.
20. Jia SF, Worth LL, Densmore CL, Xu B, Duan X, Kleinerman ES. Aerosol gene therapy with PEI: IL-12 eradicates osteosarcoma lung metastases. Clin Cancer Res 2003;9:3462–8.
21. Jia SF, Worth LL, Kleinerman ES. A nude mouse model of human osteosarcoma lung metastases for evaluating new therapeutic strategies. Clin Exp Metastasis 1999;17:501–6.
22. Duan X, Jia SF, Koshkina N, Kleinerman ES. Intranasal interleukin-12 gene therapy enhanced the activity of ifosfamide against osteosarcoma lung metastases. Cancer 2006;106:1382–8.
23. Gordon N, Koshkina NV, Jia SF, et al. Corruption of the Fas pathway delays the pulmonary clearance of murine osteosarcoma cells, enhances their metastatic potential, and reduces the effect of aerosol gemcitabine. Clin Cancer Res 2007;13:4503–10.
24. Hakkarainen T, Hemminki A, Curiel DT, Wahlfors JA. Conditionally replicative adenovirus that codes for a TK-GFP fusion protein (Ad5Δ24TK-GFP) for evaluation of the potency of oncolytic virotherapy combined with molecular chemotherapy. Int J Mol Med 2006;18:751–9.
25. Määttä AM, Liimatainen T, Wahlfors T, et al. Evaluation of cancer virotherapy with attenuated replicative Semliki forest virus in different rodent tumor models. Int J Cancer 2007;121:863–70.
26. Määttä AM, Tenhunen A, Pasanen T, et al. Non-small cell lung cancer as a target disease for herpes simplex type 1 thymidine kinase-ganciclovir gene therapy. Int J Oncol 2004;24:943–9.
27. Pasanen T, Hakkarainen T, Timonen P, et al. TK-GFP fusion gene virus vectors as tools for studying the features of HSV-TK/ganciclovir cancer gene therapy *in vivo*. Int J Mol Med 2003;12:525–31.
28. Berlin Ö, Samid D, Donthineni-Rao R, Akeson W, Amiel D, Woods VL, Jr. Development of a novel spontaneous metastasis model of human osteosarcoma transplanted orthotopically into bone of athymic mice. Cancer Res 1993;53:4890–5.
29. Loimas S, Wahlfors J, Jänne J. Herpes simplex virus thymidine kinase-green fluorescent protein fusion gene: new tool for gene transfer studies and gene therapy. Biotechniques 1998;24:614–8.
30. Duncan SJ, Gordon FC, Gregory DW, et al. Infection of mouse liver by human adenovirus type 5. J Gen Virol 1978;40:45–61.
31. Ginsberg HS, Moldawer LL, Sehgal PB, et al. A mouse model for investigating the molecular pathogenesis of adenovirus pneumonia. Proc Natl Acad Sci U S A 1991;88:1651–5.
32. Thomas MA, Spencer JF, La Regina MC, et al. Syrian hamster as a permissive immunocompetent animal model for the study of oncolytic adenovirus vectors. Cancer Res 2006;66:1270–76.
33. Sundaram M, McGuire MH, Herbold DR. Magnetic resonance imaging of osteosarcoma. Skeletal Radiol 1987;16:23–9.
34. Hellwinkel OJ, Muller J, Pollmann A, Kabisch H. Osteosarcoma cell lines display variable individual reactions on wildtype p53 and Rb tumour-suppressor transgenes. J Gene Med 2005;7:407–19.
35. Douglas JT, Kim M, Sumerel LA, Carey DE, Curiel DT. Efficient oncolysis by a replicating adenovirus (Ad) *in vivo* is critically dependent on tumor expression of primary Ad receptors. Cancer Res 2001;61:813–7.
36. Zhang Y, Bergelson JM. Adenovirus receptors. J Virol 2005;79:12125–31.
37. Witlox AM, Van Beusechem VW, Molenaar B, et al. Conditionally replicative adenovirus with tropism expanded towards integrins inhibits osteosarcoma tumor growth *in vitro* and *in vivo*. Clin Cancer Res 2004;10:61–7.
38. Suzuki K, Alemany R, Yamamoto M, Curiel DT. The presence of the adenovirus E3 region improves the oncolytic potency of conditionally replicative adenoviruses. Clin Cancer Res 2002;8:3348–59.
39. Määttä A-M. Development of Gene and Virotherapy Against Non-Small Cell Lung Cancer [dissertation]. Department of Biotechnology and Molecular Medicine. Kuopio (Finland): University of Kuopio; 2007.
40. Rautsi O, Lehmusvaara S, Salonen T, et al. Type I interferon response against viral and non-viral gene transfer in human tumor and primary cell lines. J Gene Med 2007;9:122–35.
41. Landis H, Simon-Jodicke A, Kloti A, et al. Human MxA protein confers resistance to Semliki Forest virus and inhibits the amplification of a Semliki Forest virus-based replicon in the absence of viral structural proteins. J Virol 1998;72:1516–22.
42. Morris A, Tomkins PT, Maudsley DJ, Blackman M. Infection of cultured murine brain cells by Semliki Forest virus: effects of interferon-α β on viral replication, viral antigen display, major histocompatibility complex antigen display and lysis by cytotoxic T lymphocytes. J Gen Virol 1987;68:99–106.
43. Fleming P. Age-dependent and strain-related differences of virulence of Semliki Forest virus in mice. J Gen Virol 1977;37:93–105.
44. Kaluza G, Lell G, Reinacher M, Stitz L, Willems WR. Neurogenic spread of Semliki Forest virus in mice. Arch Virol 1987;93:97–110.
45. Hefti HP, Frese M, Landis H, et al. Human MxA protein protects mice lacking a functional α/β interferon system against La crossi virus and other lethal viral infections. J Virol 1989;63:4653–64.
46. Klein MJ, Siegal GP. Osteosarcoma: anatomic and histologic variants. Am J Clin Pathol 2006;125:555–81.
47. Gisselsson D, Björk J, Höglund M, et al. Abnormal nuclear shape in solid tumors reflects mitotic instability. Am J Pathol 2001;158:199–206.
48. Witlox MA, Van Beusechem VW, Grill J, et al Epidermal growth factor receptor targeting enhances adenoviral vector based suicide gene therapy of osteosarcoma. J Gene Med 2002;4:510–6.
49. Khanna C, Prehn J, Yeung C, Caylor J, Tsokos M, Helman L. An orthotopic model of murine osteosarcoma with clonally related variants differing in pulmonary metastatic potential. Clin Exp Metastasis 2000;18:261–71.
50. Vajanto I, Rissanen TT, Rutanen J, et al. Evaluation of angiogenesis and side effects in ischemic rabbit hindlimbs after intramuscular injection of adenoviral vectors encoding VEGF and LacZ. J Gene Med 2002;4:371–80.
51. Lundström JO. Mosquito-borne viruses in Western Europe: a review. J Vector Ecol 1999;24:1–39.
52. Adekolu-John EO, Fagbami AH. Arthropod-borne virus antibodies in sera of residents of Kainji Lake Basin, Nigeria 1980. Trans R Soc Trop Med Hyg 1983;77:149–51.
53. Kokernot RH, Casaca VM, Weinbren MP, McIntosh BM. Survey for antibodies against arthropod-borne viruses in the sera of indigenous residents of Angola. Trans R Soc Trop Med Hyg 1965;59:563–70.

Oncolytic Semliki Forest Virus Vector as a Novel Candidate against Unresectable Osteosarcoma

Anna Ketola, Ari Hinkkanen, Felicitas Yongabi, et al.

Cancer Res 2008;68:8342-8350.